Electronic Supplementary Information

Engineering structural defects into a covalent organic framework for enhanced photocatalytic activity

Jixian Wang,[a] Xin-Xin Tian,[a] Lei Yu,[b] David J. Young,*[c] Wen-Bao Wang,[b] Hai-Yan Li[a] and Hong-Xi Li*[a]

[a] College of Chemistry, Chemical Engineering and Materials Science, Soochow University, Suzhou 215123, China.

[b] Analysis and Testing Centre, Soochow University, Suzhou 215123, China

[c] College of Engineering, IT and Environment, Charles Darwin University, Darwin, NT 0909, Australia.

Table of Contents

Experimental Section

Synthesis of 1,3,5-tris-(4-aminophenyl) triazine (TAPT): TAPT was synthesized according to a literature procedure with a slight modification. 4-Aminebenzonitile (6.5 mmol) was added into a Schlenk flask, which was evacuated under vacuum and filled with nitrogen. $CHCl_3$ (5 mL) was then added and the solution cooled in an ice-bath. CF_3SO_3H (1.5 mL) was added and the reaction stirred for 24 h at room temperature. Distilled water was then added and the mixture was neutralized with NaOH solution.[S1] The pale-yellow product was collected and washed with deionized water several times (Yield: 90%). ^{1}H NMR (400 MHZ, DMSO-d_6, ppm) δ 8.34 (d, J = 8.3 Hz, 6H), 6.68 (d, J = 8.4 Hz, 6H), 5.92(s, 6H), ^{13}C NMR (101 MHz, DMSO-d_6, ppm) δ = 169.6, 153.2, 130.2, 122.4, 112.6.

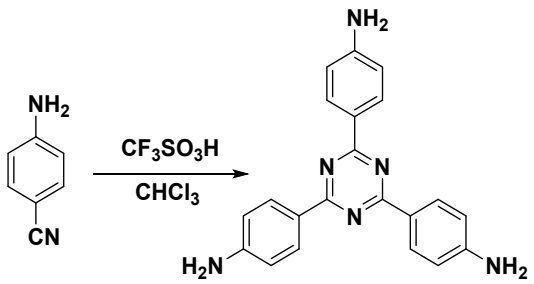

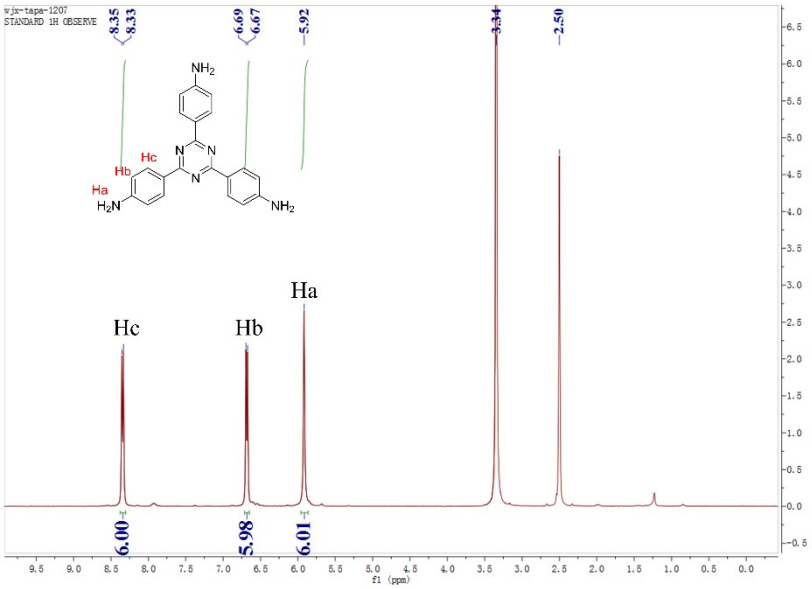

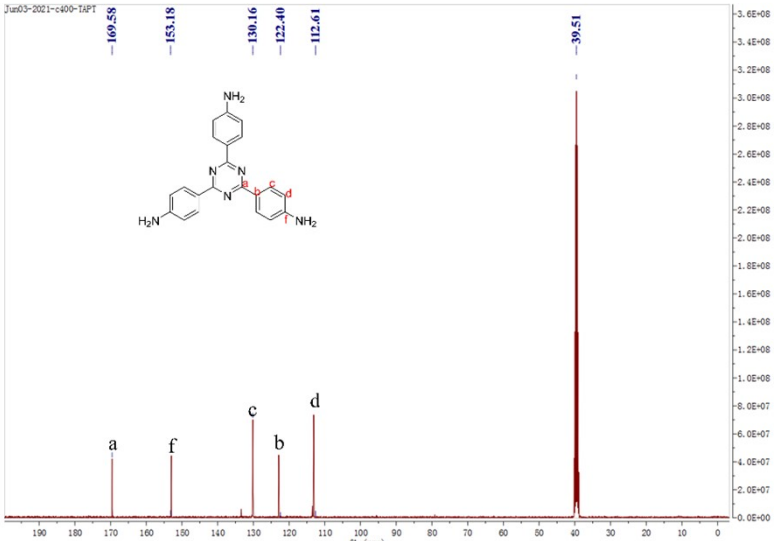

Apparent Quantum Efficiency (AQE) Measurements: The apparent quantum efficiency (AQE) for hydrogen evolution was measured under the illumination of a 300 W Xe lamp with different bandpass filters of 420 ± 10 nm, 500 ± 10 nm, 520 ± 10 nm, 550 ± 10 nm with intensities of 2.25, 2.97, 2.60 and 3.47 mW·cm^{-2}, respectively. TAPT-COF or TAPT-COF-7 was suspended in an aqueous solution of 45 mL H_2O, 5 mL TEOA and 3wt% Pt. The irradiation area was controlled to be 3.14 × 3.0^2 cm^2. The AQE was calculated according to the following Eq:[S2]

$$\eta_{AQE} = \frac{N_e}{N_p} * 100\%$$

$$= \frac{2 * n * N_A}{\frac{E_{total}}{E_{photon}}} * 100\%$$

$$E_{total} = S * P * t$$

$$E_{photon} = h * \frac{c}{\lambda}$$

$$\eta_{AQE} = \frac{2 * n * N_A * h * c}{S * P * t * \lambda} * 100\%$$

where N_e is the number of generated electrons for H_2, N_p is the number of incident photons, n is the mol. of H_2 molecules produced over 1 hour, N_A is Avogadro constant (6.022 × 10^{23} mol^{-1}), h is Planck's constant (6.626 × 10^{-34} J·s), c is the speed of light (3 ×10^8 m·s^{-1}), S is the irradiation area (m^2), P is the intensity of irradiation light (W·m^{-2}), t is the photoreaction time (t = 3600 s) and λ is the wavelength of the monochromatic light (m).

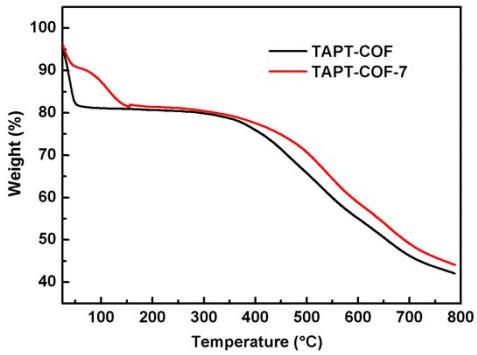

Fig. S1 TGA curves of TAPT-COF and TAPT-COF-7.

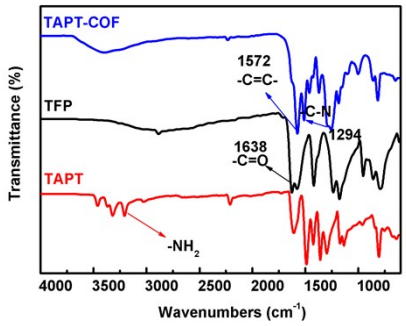

Fig. S2 FT-IR spectra of TAPT, TFP and TAPT-COF

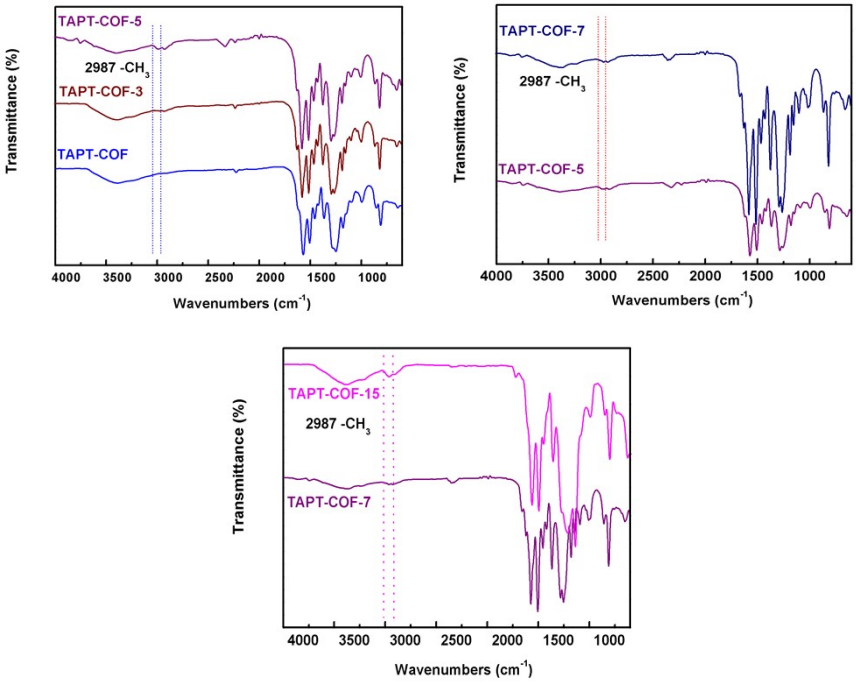

Fig. S3 FT-IR spectra of TAPT-COF-X.

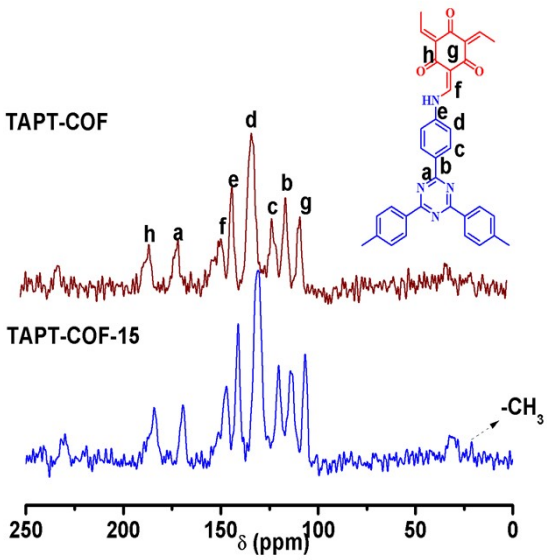

Fig. S4 Solid-state ^{13}C NMR spectra of TAPT-COF and TAPT-COF-15.

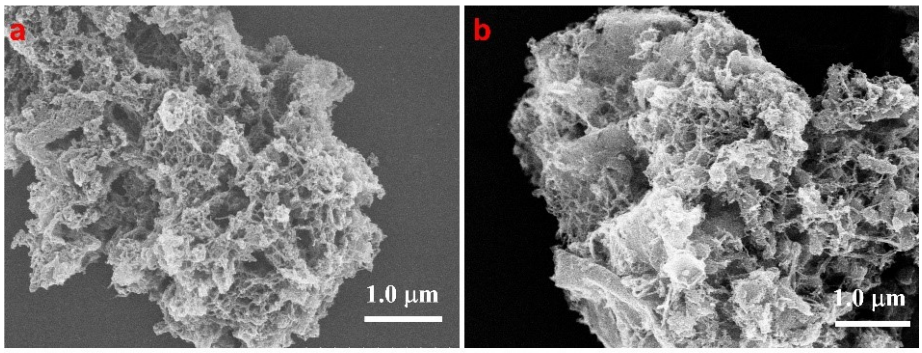

Fig. S5 SEM images of TAPT-COF (a) and TAPT-COF-7 (b).

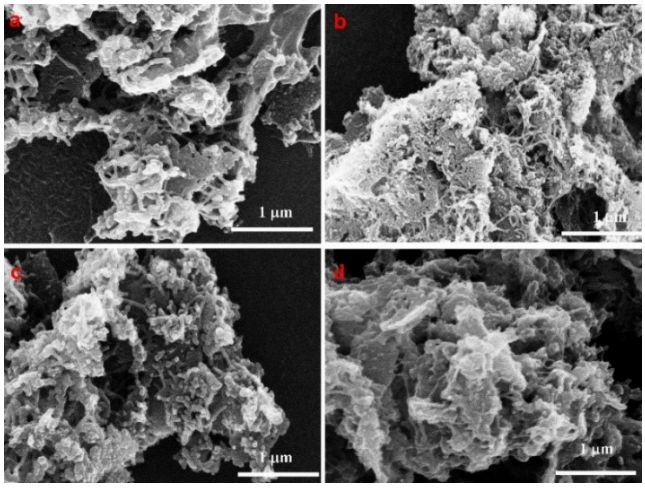

Fig. S6 SEM images of TAPT-COF-X (X = 3, 5, 10, 15).

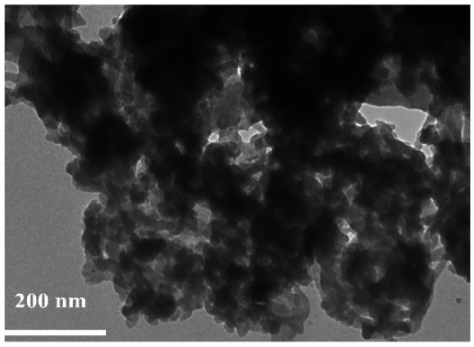

Fig. S7 TEM image of TAPT-COF.

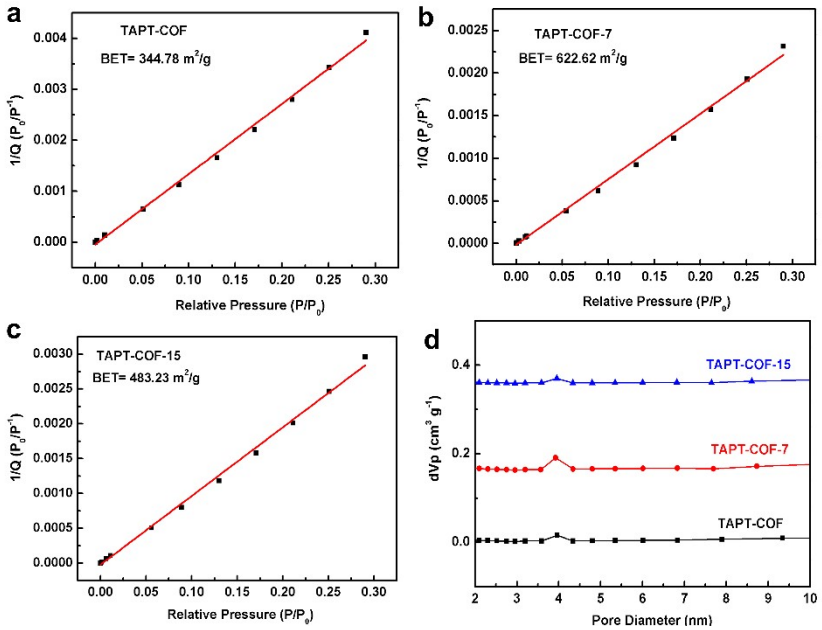

Fig. S8 BET plots of TAPT-COF (a), TAPT-COF-7 (b) and TAPT-COF-15 (c). Pore size distributions of TAPT-COF, TAPT-COF-7 and TAPT-COF-15 (d).

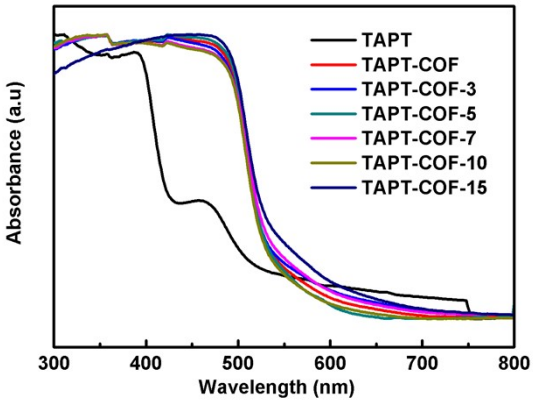

Fig. S9 UV-vis diffuse reflectance spectra (UV-DRS) of TAPT-COF-X (X = 0. 3, 5, 7, 10, 15).

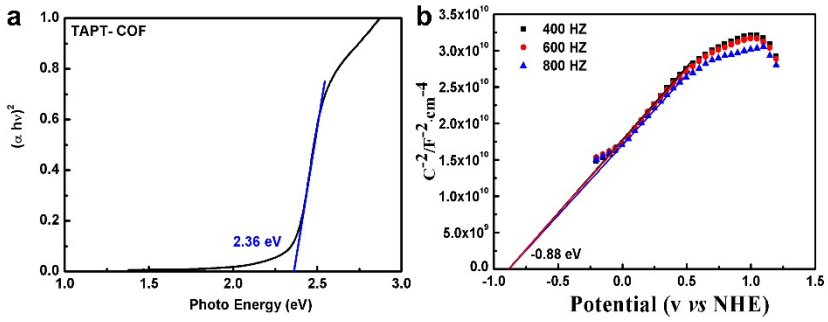

Fig. S10 Tauc and Mott-Schottky plots of TAPT-COF.

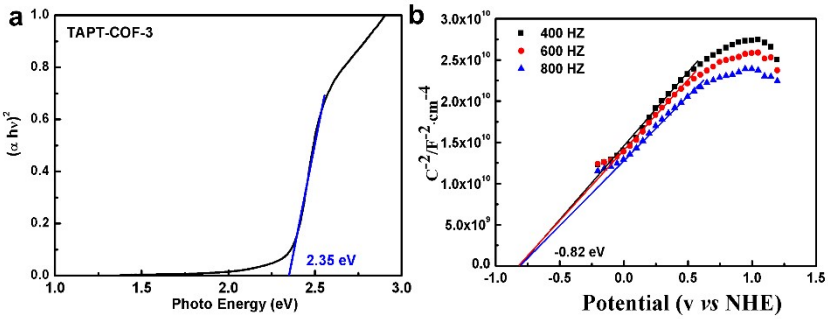

Fig. S11 Tauc and Mott-Schottky plots of TAPT-COF-3.

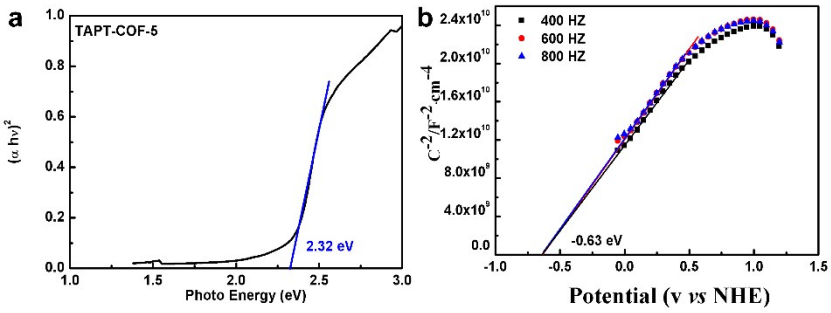

Fig. S12 Tauc and Mott-Schottky plots of TAPT-COF-5.

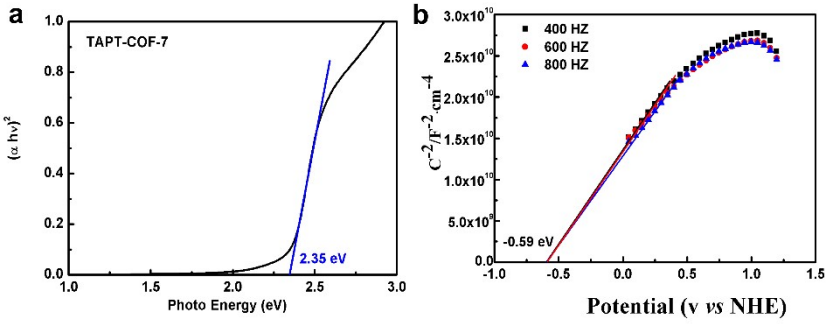

Fig. S13 Tauc and Mott-Schottky plots of TAPT-COF-7.

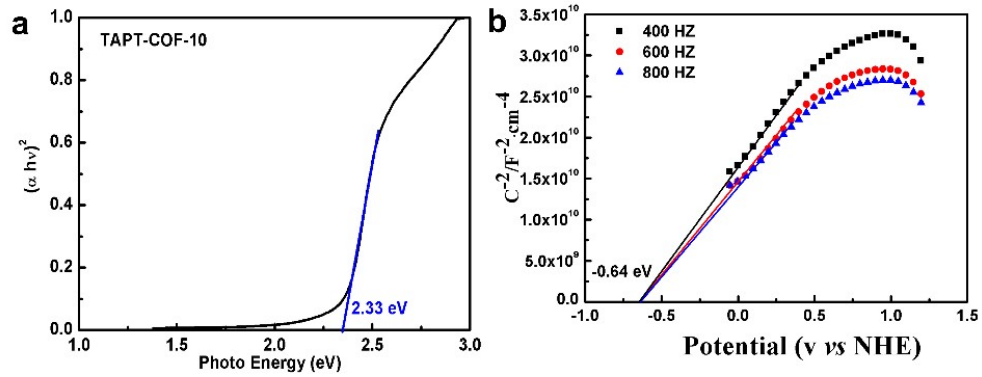

Fig. S14 Tauc and Mott-Schottky plots of TAPT-COF-10.

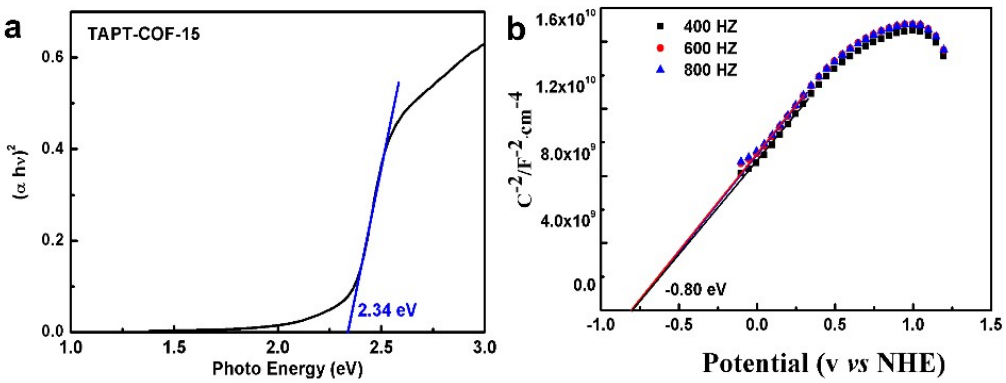

Fig. S15 Tauc and Mott-Schottky plots of TAPT-COF-15.

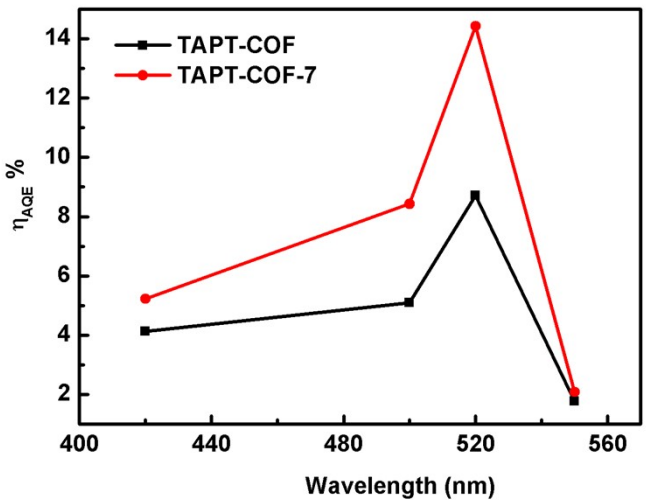

Fig. S16 Apparent quantum efficiencies (AQE) of TAPT-COF and TAPT-COF-7.

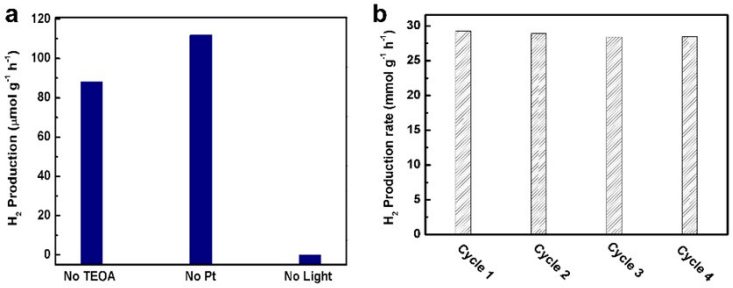

Fig. S17 Control experiments conducted in the absence of TEOA, Pt co-catalyst or light (a). The photostability of TAPT-COF-7 (5 hours is a cycle) (b).

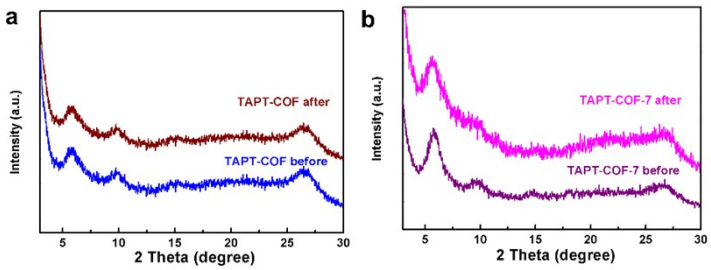

Fig. S18 PXRD patterns of TAPT-COF (a) and TAPT-COF-7 (b) before and after photocatalysis.

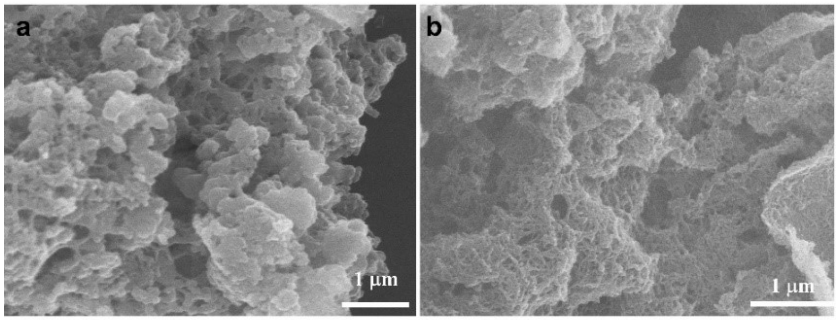

Fig. S19 SEM images of TAPT-COF (a) and TAPT-COF-7 (b) after photocatalysis.

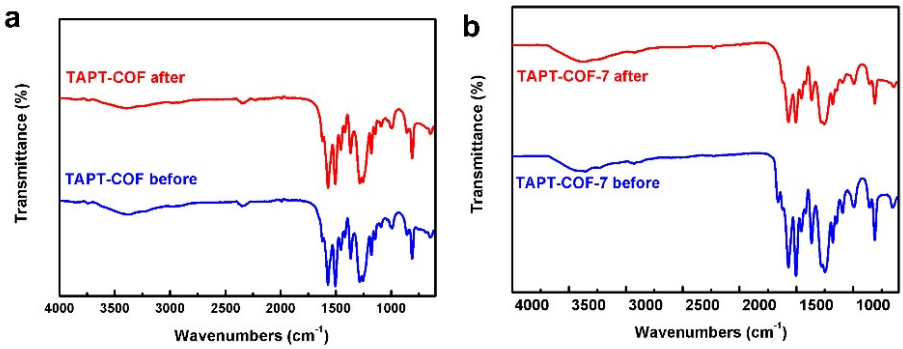

Fig. S20 FT-IR spectra of TAPT-COF (a) and TAPT-COF-7 (b) after photocatalysis.

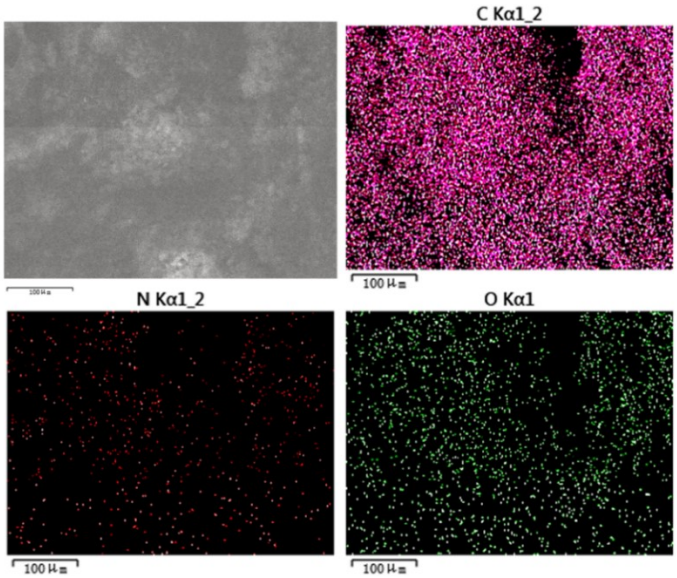

Fig. S21 EDS mapping of TAPT-COF-7 before the photocatalytic reaction.

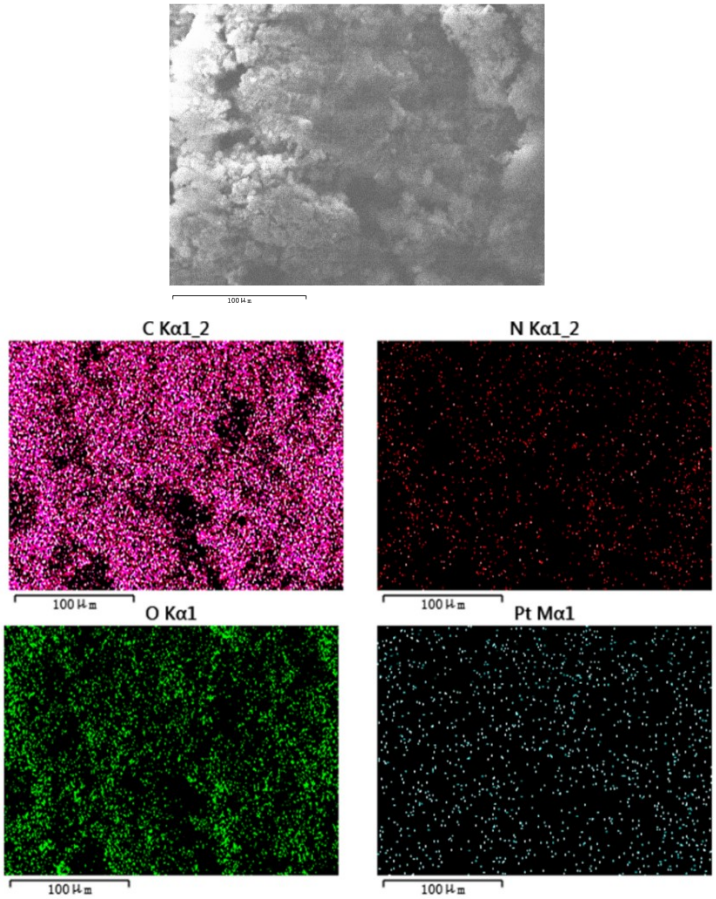

Fig. S22 EDS mapping of TAPT-COF-7 after the photocatalytic reaction.

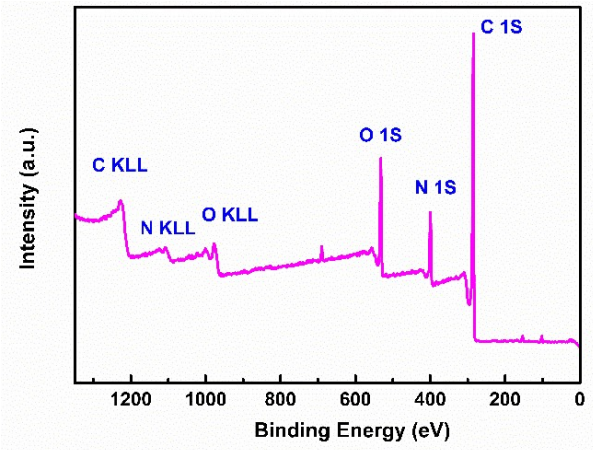

Fig. S23 Full XPS spectra of TAPT-COF-7 before the photocatalytic reaction.

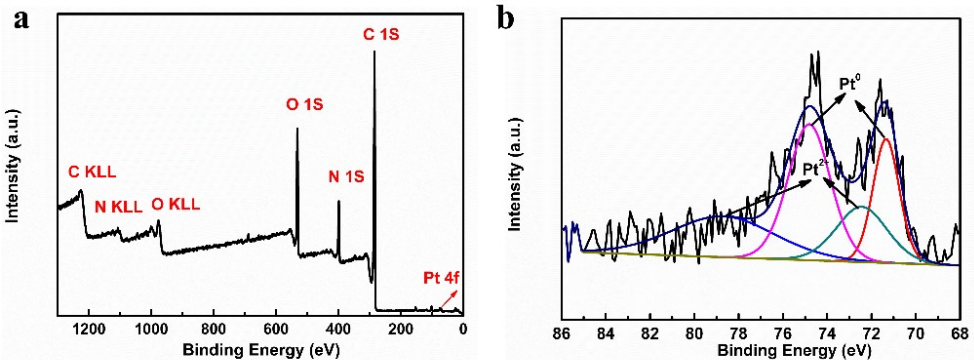

Fig. S24 Full XPS spectra and high-resolution Pt 4f XPS spectra of TAPT-COF-7 after the photocatalytic reaction.

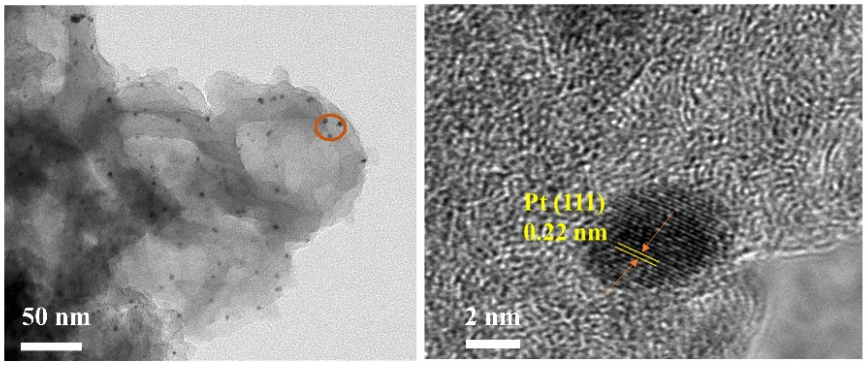

Fig. S25 HRTEM images of TAPT-COF-7 after the photocatalytic reaction.

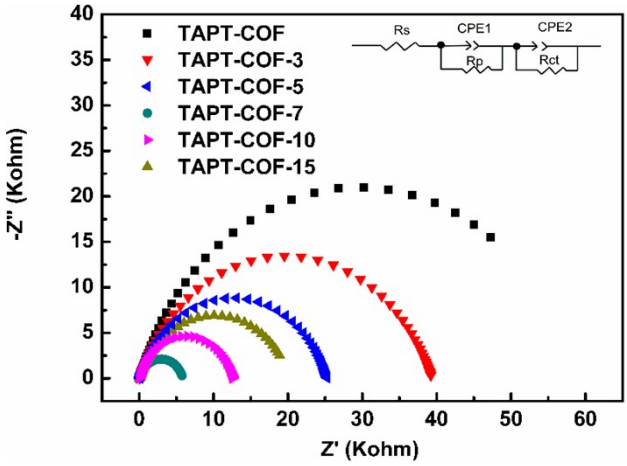

Fig. S26 Electrochemical impedance spectroscopy spectra of TAPT-COF-X.

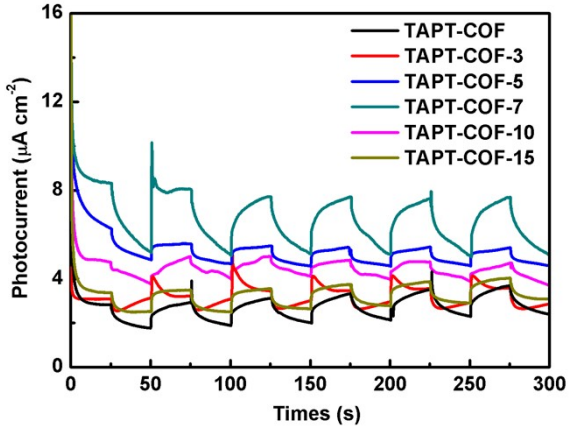

Fig. S27 Transient photocurrent curves of TAPT-COF-X

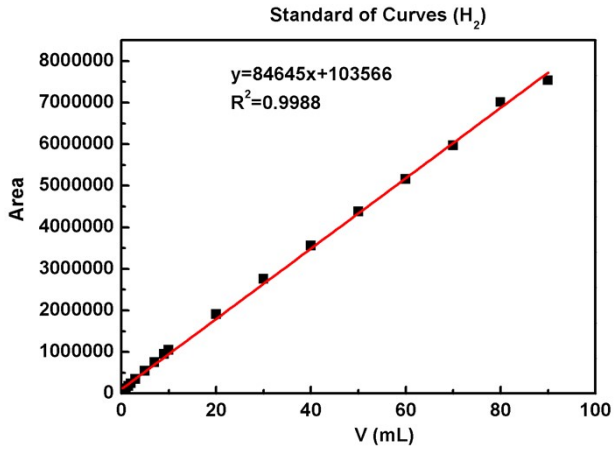

Fig. S28 Standard curve for hydrogen analysis.

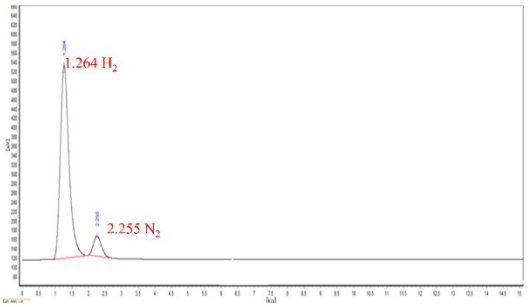

Hydrogen production results

Compound Name	R. Time (min)	Height (uV)	Area (uV*s)	Area%	Conc. (%)
H_2	1.264	413263	7564087	91.2025	91.2025
N_2	2.255	42923	729644	8.7975	8.7975
Total:		456186	8293731	100.00	100.00

Fig. S29 GC trace for TAPT-COF-7 at 5h.

Table S1. Comparison of photocatalytic HER performance of reported 2D COFs

Photocatalyst	Linkages	SED	Activity ($\mu mol\ g^{-1}\ h^{-1}$)	Ref
TFPT-COF	Hydrazone	sodium ascorbate	1970	S4
N3-COF	Azine	TEOA	1703	S5
TP-BDDA COF	Imine	TEOA	324	S6
FS-COF	β-ketoenamine	ascorbic acid	10100	S7
Tapa-COF-$(CH_3)_2$	β-ketoenamine	Sodium ascorbate	8330	S8
NTU-BDA-THAT	β-ketoenamine	ascorbic acid	1127.1	S9
NH_2-Mexene (8:4)*	/	ascorbic acid	14288.1	S9
MoS_2/TpPa-1-COF*	/	ascorbic acid	5885	S10
TiO_2-TpPa-1-COF	/	Sodium ascorbate	11190	S11
NH_2-UiO-66/TpPa-1-COF	/	Sodium ascorbate	23410	S12
sp^2C-COF_{ERDN}	sp^2 carbon-conjugated	TEOA	2120	S13
TAPT-COF-7	β-ketoenamine	TEOA	33910	This Work

* Without Pt nanoparticles as Co-catalyst.

References

S1 B. C. Patra, S. K. Das, A. Ghosh, A. Raj K, P. Moitra, M. Addicoat, S. Mitra, A. Bhaumik, S. Bhattacharya and A. Pradhan, *J. Mater. Chem. A.*, 2018, **6**, 16655-16663.

S2 Z. Zhao, Y. Zheng, C. Wang, S. Zhang, J. Song, Y. Li, S. Ma, P. Cheng, Z. Zhang and Y. Chen, *ACS Catal.*, 2021, **11**, 2098-2107.

S3 L. Stegbauer, K. Schwinghammer and B. V. Lotsch, *Chem. Sci.*, 2014, **5**, 2789-2793.

S4 V. S. Vyas, F. Haase, L. Stegbauer, G. Savasci, F. Podjaski, C. Ochsenfeld and B. V. Lotsch, *Nat. Commun.*, 2015, **6**, 8508.

S5 P. Pachfule, A. Acharjya, J. Roeser, T. Langenhahn, M. Schwarze, R. Schomacker, A. Thomas and J. Schmidt, *J. Am. Chem. Soc.*, 2018, **140**, 1423-1427.

S6 X. Wang, L. Chen, S. Y. Chong, M. A. Little, Y. Wu, W. H. Zhu, R. Clowes, Y. Yan, M. A. Zwijnenburg, R. S. Sprick and A. I. Cooper, *Nat. Chem.*, 2018, **10**, 1180-1189.

S7 J. L. Sheng, H. Dong, X. B. Meng, H. L. Tang, Y. H. Yao, D. Q. Liu, L. L. Bai, F. M. Zhang, J. Z. Wei and X. J. Sun, *ChemCatChem*, 2019, **11**, 2313-2319.

S8 H. Wang, C. Qian, J. Liu, Y. Zeng, D. Wang, W. Zhou, L. Gu, H. Wu, G. Liu and Y. Zhao, *J. Am. Chem. Soc.*, 2020, **142**, 4862-4871.

S9 M.-Y. Gao, C.-C. Li, H.-L. Tang, X.-J. Sun, H. Dong and F.-M. Zhang, *J. Mater. Chem. A*, 2019, **7**, 20193-20200.

S10 C.-C. Li, M.-Y. Gao, X.-J. Sun, H.-L. Tang, H. Dong and F.-M. Zhang, *Appl. Catal. B Environ.*, 2020, **266**, 118586.

S11 F. M. Zhang, J. L. Sheng, Z. D. Yang, X. J. Sun, H. L. Tang, M. Lu, H. Dong, F. C. Shen, J. Liu and Y. Q. Lan, *Angew. Chem. Int. Ed.*, 2018, **57**, 12106-12110.

S12 E. Jin, Z. Lan, Q. Jiang, K. Geng, G. Li, X. Wang and D. Jiang, *Chem*, 2019, **5**, 1632-1647.